Direct Fluorescence Technique to Study Evolution in Transparency and Crossing Density at Polymer–Polymer Interface During Film Formation from High-T Latex Particles

Ö. PEKCAN* and M. CANPOLAT

Department of Physics, Istanbul Technical University, Maslak, 80626, Istanbul, Turkey

SYNOPSIS

The Direct Fluorescence method was used to study the healing process during latex film formation above the glass transition temperature. The latex film was prepared from pyrene (P)-labeled poly(methyl methacrylate) (PMMA) particles. Heptane was used as a mixing agent. The steady-state fluorescence technique was employed to measure the density of polymer chains crossing the particle–particle interface. Various latex films with different latex content were used to study the transparency below and above the healing temperature. Crossing density was found to depend linearly on $(\text{time})^{1/2}$, which was proposed by Prager and Tirrell. © 1996 John Wiley & Sons, Inc.

INTRODUCTION

Aqueous dispersions of colloidal particles with glass transition temperature (T_g) below the drying temperature are called low-T latex dispersions; however, aqueous or nonaqueous dispersions of colloidal particles where T_g exceeds the drying temperature are generally named high-T latex dispersions. When aqueous dispersion of low-T latex particles is coated onto a substrate and the solvent is allowed to evaporate, initially a white, opaque film is formed. At the early stage of film formation, once sufficient solvent has evaporated, the particles come into contact and begin to deform.[1,2] Deformation is driven by a combination of surface and osmotic forces, and resisted by the elastic modules of the latex.[1] However high-T latex particles remain essentially discrete and undeformed during drying. The mechanical properties of these films continue to evolve long after all the solvent has evaporated. This process of further coalescence is an important aspect of all latex coatings and represents an important feature that one would like to understand. Further coalescence can also be achieved by annealing the latex film. The mechanism of film formation is know as interdiffusion of polymer chains followed by healing at the particle–particle interface.

In general, when two identical polymeric materials are brought into intimate contact and heated at a temperature above the glass transition, the polymer chains become mobile and interdiffusion of polymer chains across the interface can occur. After this process, the junction surface becomes indistinguishable in all respects from any other surface that might be located in the polymeric material. This process is called healing of the junction, where the joint achieves the same cohesive strength as the bulk polymeric material.

In the bulk state, polymer chains have a Gaussian distribution of segments. Chains confined to the half space adjacent to the junction have distorted conformations.[3,6] Diffusion across the junction leads to configurational relaxation and recovery of Gaussian chain behavior. Polymers much larger than a certain length are often pictured as confined to a tube, and diffusion occurs by a reptile-like motion. In this model, each polymer chain is considered to be confined to a tube, along the length of which it executes a random back and forth motion. This reptile-like motion will cause the chain to slip out of a section of tube at one end or the other. The reptation time, T_R, describes the time necessary for a polymer to

* To whom correspondence should be addressed.

Journal of Applied Polymer Science, Vol. 59, 277–285 (1996)
 CCC 0021-8995/96/020277-09

diffuse a sufficient distance for all memory of the initial tube to be lost. This is the time it takes for the initial configuration to be forgotten and the first relaxation to be completed.

Over the last several years, it has become possible to examine latex film formation at the molecular level. Small-angle neutron scattering (SANS) allows one to examine deuterated particles in a protonated matrix.[7] Alternatively, the process of interparticle polymer diffusion has been studied by direct nonradiative energy transfer (DET) using fluorescence decay measurements in conjunction with particles labeled with appropriate donor and acceptor chromophors.[8–10] This transient fluorescence technique has been used to examine latex film formation of 1 μm diameter poly(methyl methacrylate) (PMMA) particles[8] and of 100 nm diameter poly(buthyl methacrylate) (PBMA) particles.[9,10] These studies all indicate that in the particular systems examined, annealing the films above T_g lead to polymer interdiffusion at the particle–particle junction as particle interface heals. Recently, employing DET, the steady-state fluorescence technique has been used by us to study healing and interdiffusion processes at the particle–particle junction during film formation from PMMA latex particles.[11,12] In steady-state fluorescence studies film thickness and transparency are more important than in fluorescence decay measurements during the annealing process. Before annealing, the mean free path of the photon is of the order of the size of the interparticle voids, and after a few steps the photon may reemergerge from the front surface of the film. Once the healing process is completed, the mean free path of a photon becomes of the order of the particle size and the photon may spend a longer time in the film. Special attention has to be paid to reducing these effects in the steady-state technique.

In this work we studied film formation from high-T latex particles as a function of solid content using the steady-state fluorescence technique. Direct fluorescence measurements were employed to examine healing processes during film formation of PMMA particles. The effect of transparency of the film on light absorption by the chromophore was examined before and after the healing of latex particles. Isothermal diffusion experiments were performed using the direct fluorescence method to study chain flow across the particle–particle junction. Increase in the chromophore intensity by increasing annealing time was attributed to increase in the "crossing density" at the junction. The model developed by Tirrel[4] was used to investigate the characteristics of the healing process.

The 1–3 μm diameter particles labeled with pyrene (P) and having two components were used;[13,14] the major part, PMMA, comprises 96 mol % of the material and the minor component, polyisobutylene (PIB) (4 mol %), forms an intepenetrating network through the particle interior,[15,16] very soluble in certain hydrocarbon media. A thin layer of PIB covers the particle surface and provides colloidal stability by steric stabilization.

EXPERIMENTAL

Pyrene (P)-labeled PMMA-PIB polymer particles were prepared separately in a two-step process in which MMA in the first step was polymerized to low conversion in cyclohexane in the presence of PIB containing 2% isoprene units to promote grafting. The graft copolymer so produced served as a dispersant in the second stage of polymerization, in which MMA was polymerized in a cyclohexane solution of the polymer. Details have been published previously.[13] A stable spherical dispersion of the polymer particles was produced, ranging in radius from 1 to 3 μm. A combination of ^{1}H-NMR and UV analysis indicated that these particles contain 6 mol % PIB and 0.037 mmol P groups per gram of polymer. (These particles were prepared by B. Williamson in Prof. M. A. Winnik Laboratory in Toronto, and provided to us for our use.) Latex film preparation were carried out by dispersing particles in heptane in a test tube with the solid content taken to be 0.24%.

In this work, two sets of fluorescence experiments were carried out; in the first set, 10 different film samples were prepared from the dispersion of particles by placing different number of drops on round quartz window plates with a diameter of 1.35 cm and allowing the heptane to evaporate. Here, we were careful that the liquid dispersion from droplets has to cover the whole surface area of the plate and remain there until the heptane has evaporated. Samples were weighed before and after the film casting to determine the latex contents, film thicknesses, and coverage fraction of particles in films. Here, the assumption is made that each drop contained and equal number of latex particles. Samples of high latex contents were used as references to calculate the latex content in a single droplet (=0.05 mg). Then, the latex content in each film was estimated by multiplying 0.05 mg, with the number of droplets an each sample. These values are summarized in Table I. Average size for the particles was

Table I

Latex Content (mg)	Film Thickness (μm)	Coverage Fraction (%)
0.15	0.22	15
0.30	0.44	30
0.45	0.66	44
0.60	0.88	60
0.75	1.10	74
0.90	1.32	88
1.05	1.54	103
1.20	1.76	118
1.35	1.98	133
1.50	2.20	147

Latex content in films were estimated by weighing the samples before and after the film casting. Coverage fractions were found by taking the average size of particles as 1.5 μm.

taken to be 1.5 μm to calculate the number of layers or coverage fraction of particles. For example, in the samples of 0.9 mg latex content, particles occupied almost a monolayer film.

In this set of experiments the film samples were annealed above T_g of PMMA for 0.5-h intervals at elevated temperatures up to 210° in an oven. The temperature was maintained within ± 2° during annealing. After annealing, each sample was placed in the solid surface accessory of a Model LS-50 fluorescence spectrometer (Perkin–Elmer). P was excited at 345 nm and fluorescence emission was detected between 370–440 nm. In order to test the reproducibility of data and to estimate errors, 10 different samples were used for each latex content. In this work, the source of errors originate mostly from the surface inhomogeneities of film samples, which cause variation in fluorescence intensities. Errors coming from the variation in time and temperature are negligible when compared to the errors on fluorescence intensities due to film surfaces. The signal-to-noise ratio in fluorescence intensities is also quite low (2–3%) and can be neglected in error estimations.

In the second set of experiments, isothermal fluorescence measurements were carried out by annealing two different monolayer samples separately at 120 and 160°C, at various time intervals. Fluorescence emission spectra of P of these films were measured after each annealing process.

All measurements were carried out in the front face position at room temperature. Slit widths were kept at 2.5 mm.

RESULTS AND DISCUSSION

Solid Content and Transparency of Films

Typical emission (I_{op}) and scattered (I_{sc}) spectra of a latex film after annealing at elevated temperatures for 0.5-h intervals and excited at 345 nm are shown in Figure 1. In all samples, P intensity (I_{op}) first increased and reached a maximum at 140°C, then decreased; however I_{sc} decreased continuously with increasing annealing temperature. I_{op} vs. annealing temperature is plotted in Figure 2(a,b,c) for 0.3, 1.05, and 1.5 (mg) latex content samples, respectively. The maximum in I_{op} can be explained by the healing process[11,17] at the particle–particle junction where the polymer chains try to relax across the junction surface. The time 0.5 h can be referred to as the healing time (τ_H) for the polymer at 140°C, during which the chains move halfway across the interface surface. At this temperature and time, particle boundaries start to disappear and, consequently, latex film becomes almost transparent to the exciting light for P molecules. As a result, the emission intensity, I_{op} reaches to the maximum. At 210°C; however, complete transparency is reached due to annealing of latex film. Variation in P intensity most

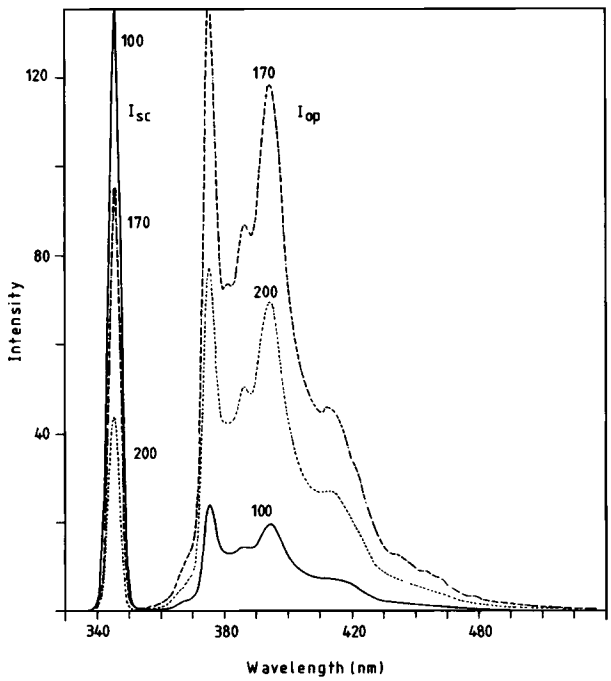

Figure 1 Emission (I_{op}) and scattered (I_{sc}) spectra of pyrene, after latex film of 0.9 mg sample annealed at 100, 170, and 200°C temperatures for 0.5-h intervals, and excited at 345 nm.

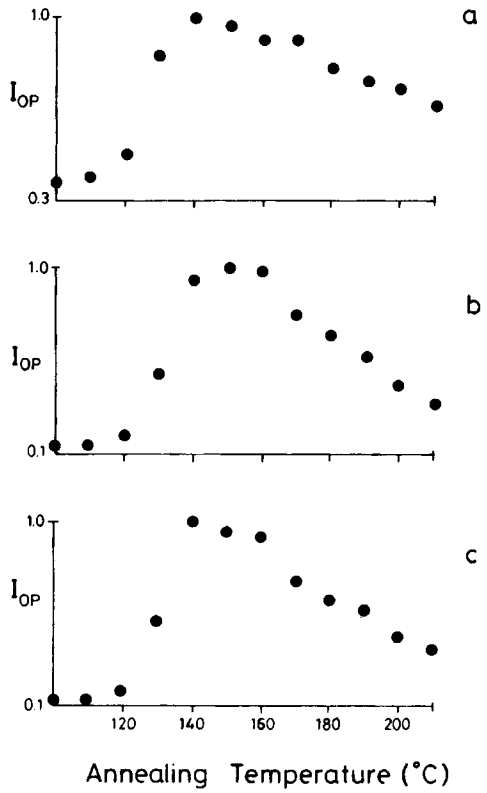

Figure 2 Variation in pyrene intensity with respect to annealing temperature in: (a) 0.30, (b) 1.05, and (c) 1.50 mg samples.

probably depends on the variation in the optical path of a photon in the film, which is shortest before annealing (films is turbid and mean free path is shortest) and after annealing is completed (film is fully transparent and mean free path becomes longest). At the healing point, however, there are some sharp boundaries, at which the photon can be refracted many times in the film and the optical path becomes longest, and probability of finding a pyrene by a photon becomes highest. These qualitative explanations can be quantified by performing Monte Carlo simulations conjunction with the photon diffusion theory (This work is an progress and will reported soon.[17])

Scanning electron microscopy (SEM) results of a annealed latex film at four different temperatures for 0.5-h intervals are presented in Figure 3. Disappearing boundaries at 140°C is shown in Figure 3(c). Complete transparency of the film is reached at 210°C, which is presented in Figure 3(d).

For a control experiment, the temperature variation of I_{op} in completely transparent films casted from chloroform solution of latex particles were measured and are presented in Figure 4(a,b). Thicknesses of these films corresponds to latex films in Figure 2(b) and 2(c), respectively. Naturally, the temperature behavior of chloroform-cast films showed no variation in transparency during annealing at elevated temperatures, indicating that the structure of these films has been already evolved during the casting process, and the optical path of a photon stays constant during the annealing processes. The slow decrease of I_{op} in Figure 4(b) for the thicker film may come from residual chloroform bubbles.

The behavior of I_{op} with respect to the latex content before and after annealing below T_g is presented in Figure 5. I_{op} intensity first increases by increasing the latex content on the quartz plate, then saturates above the 1.05 mg sample (coverage fraction is larger than 100%) due to increasing of the scattered excited light by latex film. When the films of various latex contents were annealed at 140 and 210°C, I_{op} increased in proportion to the thickness of the films. Results are shown in Figure 6, where P intensity is plotted against latex content at two different annealing temperatures. The slope of the curve for 140°C is observed to be much larger than the curve for 210°C, indicating that the complete transparency is reached at the 210°C temperature. In other words, the optical path of a photon is much shorter in annealed film at 210°C than in 140°C. A few points deviated from linearity at 140°C, a fact that may be related to the instability of healing at this temperature. However, at 210°C where film becomes completely transparent, the curve present nice linear behavior.

Cartoon representation of latex film formation processes is summarized in Figure 7 for the 1.35 mg sample where initially (a) heptane evaporates and close-packed particles form a powder film. In (b), due to healing, particle boundaries start to disappear and almost transparent film is formed. In (c), mechanically rigid, fully transparent film is formed at annealing temperature of 210°C.

Crossing Density during Film Formation

When a film sample of 1.35 mg latex content was annealed at 160°C for various periods of time, a continuous increase in I_{op} intensity was observed until it saturated above the 300 min annealing time. The result is shown in Figure 8(a). The increase in I_{op} may be explained by the increase in transparency of the latex film due to the disappearing of particle–particle boundaries. Presumably, as the annealing

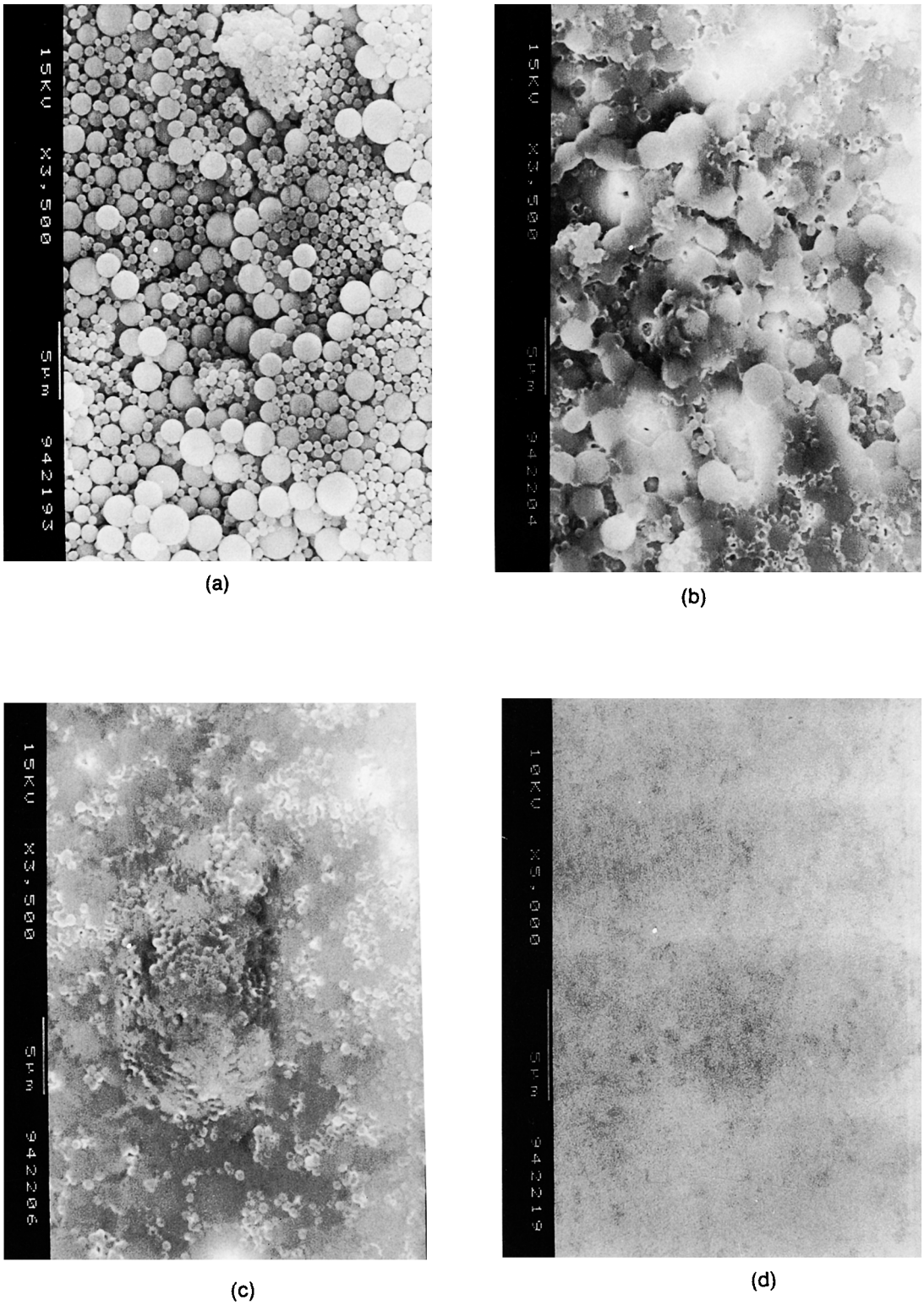

Figure 3 Scanning electron microscopy results of annealed latex film, for 0.5-h intervals: (a) 20°C, (b) 120°C, (c) 140°C, and (d) 210°C temperatures.

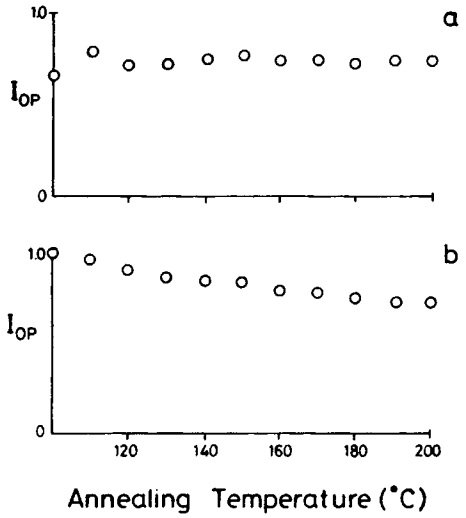

Figure 4 Variation in pyrene intensity with respect to annealing temperature of chloroform treated samples. Thicknesses correspond to latex films of (a) 1.05, (b) 1.50 mg samples in Figure 2.

time is increased, more chains cross the junction surface. As a result, some boundaries disappear and the film become almost transparent to the exciting light and the emission intensity, I_{op} increase until it saturates. Here, we have to note that at this temperature and time, the optical path of a photon is longest and the probability of finding of a pyrene by a photon is highest.

In order to quantify the above results, the Prager–Tirrel (PT) model[4] for the chain crossing density was employed. These authors used de Gennes's "reptation" model[3] to explain configurational relaxation at the polymer–polymer junction where each polymer chain is considered to be confined to a tube in which it executes a random back and forth

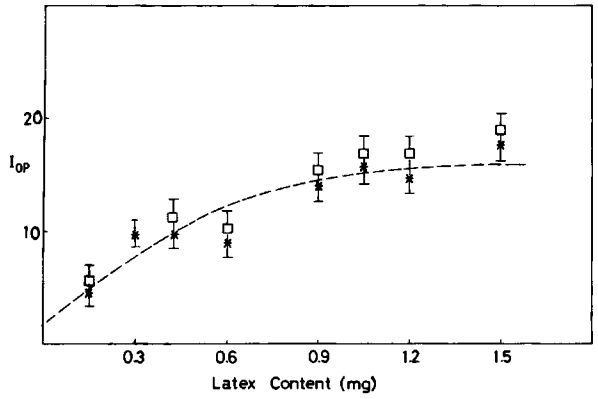

Figure 5 Plot of I_{op} vs. latex content of samples *before annealing; □ annealed at 100°C.

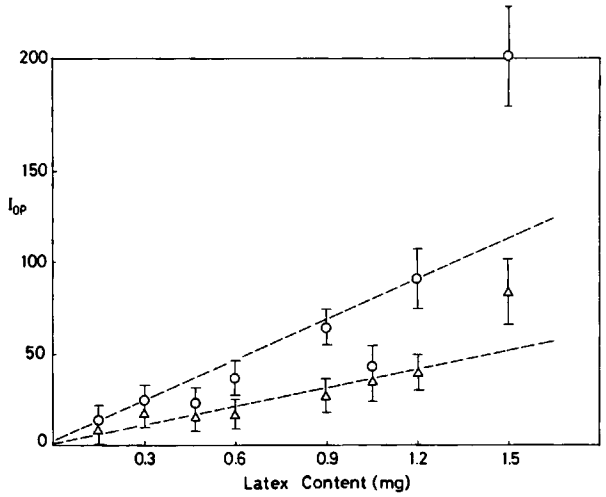

Figure 6 Plot of I_{op} vs. latex content of samples: ○ annealed at 140°C; △ annealed at 210°C.

motion. A homopolymer chain with N freely jointed segments of length was considered by PT, which moves back and forth by one segment with a frequency v. In time, the chain displaces down the tube by a number of segments, s. $v/2$ is called the "diffusion coefficient" of s in one-dimensional motion. PT calculated the probability of the net displacement with s during time t in the range of n-Δ to n-$(\Delta + d\Delta)$ segments. A Gaussian probability density was obtained for small times and large N. The total "crossing density" $\sigma(t)$ (chains per unit area) at the junction surface then was calculated from the contributions $\sigma_1(t)$ due to the chains still retaining some portion of their initial tubes, plus a remainder, $\sigma_2(t)$. Here, the $\sigma_2(t)$ contribution comes from chains that

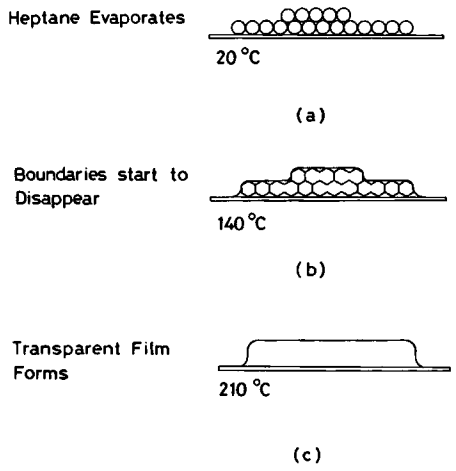

Figure 7 Cartoon representation of latex film formation process.

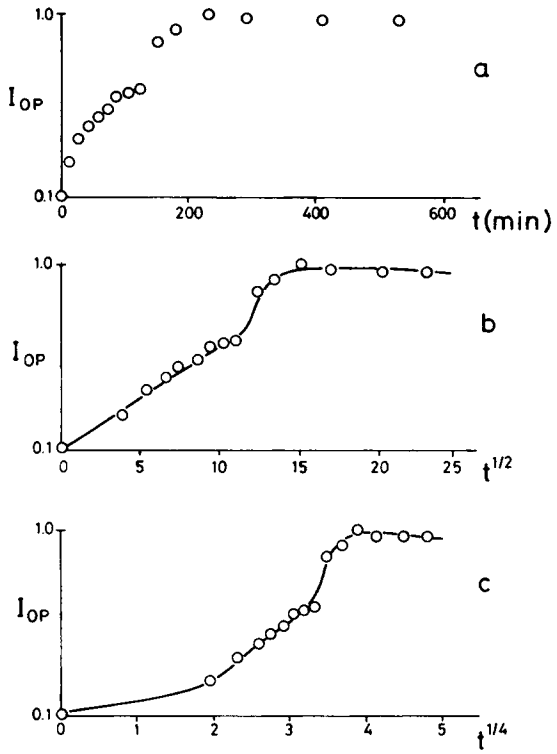

Figure 8 Plot of I_{op} vs. (a) annealing time t, (b) $t^{1/2}$, and (c) $t^{1/4}$ of sample annealed at 160°C, in various times.

have relaxed at least once. In terms of reduced time $\tau = 2vt/N^2$, the total crossing density can be written as

$$\sigma(\tau)/\sigma(\infty) = 2\pi^{-1/2}\left[\tau^{1/2} + 2\sum_{k=0}^{\infty}(-1)^n \times [\tau^{1/2}\exp(-k^2/\tau) - \pi^{-1/2}erfc\,(k/\tau^{1/2}]\right]. \quad (1)$$

For small τ values the summation term of the above equation is very small and can be neglected, which then results in

$$\sigma(\tau)/\sigma(\infty) \approx 2\pi^{-1/2}\tau^{1/2}. \quad (2)$$

This was predicted by de Gennes on the basis of scaling arguments.[3] Theoretical results from the work of PT is shown in Figure 9. In order to compare our results with the crossing density of the PT model, I_{op} was plotted against $t^{1/2}$ in Figure 8(b). At early times I_{op} increase linearly, then there is a distinct jump in I_{op} at intermediate times. As pointed out before, the increase in I_{op} can be related to the increase in transparency of the latex film due to disappearing of particle–particle boundaries. As annealing time increased, more chains relaxed across the junction surface, and as a result, the crossing density increased. Here, basically we assumed that I_{op} is directly proportional to the crossing density during film formation processes. Linear behavior of I_{op} versus $t^{1/2}$ at early times might be related to the $\sigma_1(t)$ term in the PT model, which comes from the chains still retaining a portion of their initial tube. However, at intermediate times the term $\sigma_2(t)$ becomes significant and $\sigma_1(t)$ reaches its maximum, which causes a jump in the I_{op} intensity. Our experimental results in Figure 8(b) is consistent with the PT's theoretical predictions in Figure 9, where $\sigma(t)$ shows a jump at intermediate times. In the long time limit, where chains have relaxed more than once, I_{op} saturates in time, in accordance with PT's prediction.

PT have shown[3] that when the initial segment distribution of polymer chains is not uniform, then the total crossing density at short times can be given as

$$\sigma(t) \approx \sigma_1(t) \approx 0.004\rho_o(vt)^{1/4}, \quad (3)$$

where ρ_o is the initial surface density of terminal segments at the junction. To test the reliability of eq. (3), I_{op} is plotted against $t^{1/4}$ in Figure 8(c),

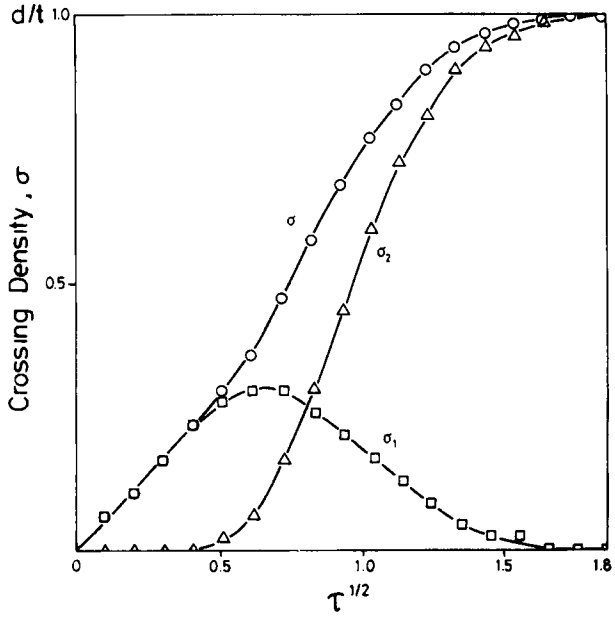

Figure 9 Theoretical results of crossing density obtained by Prager and Tirrell from Ref. 4. $\sigma(t)$ is the total crossing density, $\sigma_1(t)$ is the crossing density from chains that still retain a portion of their initial tube, $\sigma_2(t)$ is from all other chains.

which gives very bad linear relation, indicating that the segmental distribution at the particle–particle interface is quite uniform.

When the latex film was annealed just above T_g of PMMA, at 120°C, very slow variation was observed in I_{op} against t. The variation of I_{op} vs. t, $t^{1/2}$, and $t^{1/4}$ were plotted in Figure 10(a–c), respectively. As expected, a linear relation was observed between I_{op} and $t^{1/2}$ at early times, and the characteristic jump was detected at intermediate region. The $t^{1/4}$ dependence of I_{op} showed poor linear relation, which supports the similar behavior at 160°C experiment.

The Temperature dependence of I_{op}, which is proportional to $\sigma(\tau)/\tau(\infty)$ can be quantified using eq. (2) by assuming the Arrhenius relation for the linear diffusion coefficient, $v = v_o \exp(-\Delta E/kT)$. Then, for lower temperatures, $\sigma(\tau)$ varies slowly in time, as shown in Figure 10(a). When the annealing temperature is increased, then more chains can be relaxed across the junction surface and I_{op} varies faster in time, as presented in Figure 7(a). v^{-1} values were estimated at short times from the slopes of Figures 8(b) and 10(b) and found to be $\nu_1^{-1} = 24$ s and $\nu_1^{-1} = 2.7$ s, respectively. Equation (2) was used, and the number of segments was taken to be $N = 500$ to get the above results.

Here, ν_1^{-1} and $\nu_2 - 1$ values can be associated with short-range wriggling motions of the polymer chain in the tube at 160 and 120°C temperatures, respectively. When these characteristic times are compared with the healing times (τ_H) at the corresponding temperatures[18] (15 min and 180 min), it is seen that τ_H values are much larger than wriggling times, which is quite reasonable from the point of view that healing times are comparable to the tube renewal times (T_R).[4,5]

In the Arrhenius relation v, when the ΔEs are taken to be healing ($\Delta E_H = 9.84$ kcal/mol) and diffusion ($\Delta E_p = 30$ kcal/mol) activation energies,[12,18] the corresponding v_1/v_2 ratios can be found at 2.7 and 27.1, respectively. When these ratios are compared with the v_1/v_2 ratio, which was obtained in this article ($v_1/v_2 = 11.1$), one can argue that the activation energy needed for the chain segments responsible for the $\sigma_1(t)$ contribution should be larger than ΔE_H but smaller than ΔE_p. In other words, the activation energy in the $\sigma_1(t)$ term of the crossing density is responsible for a larger amount of segments crossing the junction surface than the healing activation energy, which is responsible for the minor chains crossing the same surface area.[19] However, the activation energy in the $\sigma_2(t)$ term can be taken as ΔE_p, because the $\sigma_2(t)$ contribution to the crossing density comes from the chains, which have relaxed at least once.

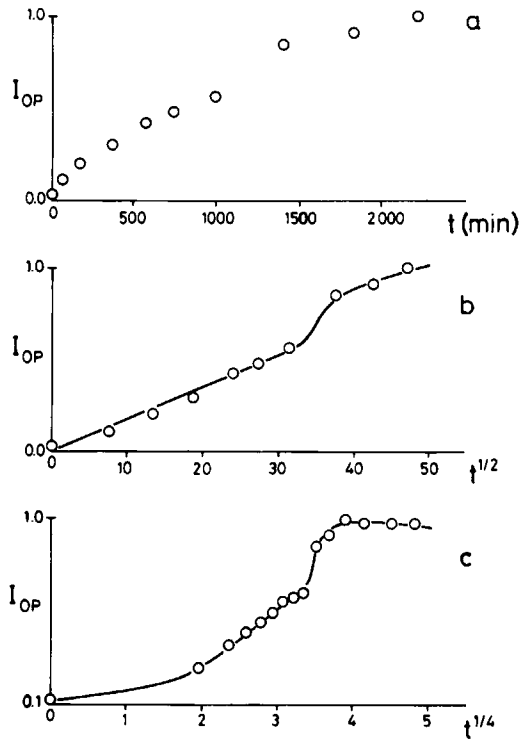

Figure 10 Same as in Figure 7, but sample annealed at 120°C.

In these experiments, time and temperature for studying healing processes are found to be very critical. One has to be careful in choosing the annealing time at a given temperature. This particular time has to be comparable with the relaxation time of the polymer chain to observe the details of the healing process.[18] For higher temperatures, smaller time intervals have to be chosen to detect the chain relaxation across the junction surface; for lower temperatures, however, longer time intervals are needed to observe the same effects.

We are grateful to TUBA (Turkish Academy of Sciences) for their financial assistance and thank to Professor M. A. Winnik for supplying us with the latex material and documents to read.

REFERENCES

1. S. T. Eckersley and A. Rudin, *J. Coat. Technol.*, **62**, No.780, 89 (1990).

2. M. Joanicot, K. Wong, J. Maquet, Y. Chevalier, C. Pichot, C. Graillat, P. Linder, L. Rios, and B. Cabane, *Prog. Colloid Polym. Sci.,* **81,** 175 (1990).
3. P. G. de Gennes, *C.R. Acad. Sci. (Paris),* **291,** 219 (1980).
4. S. Prager and M. Tirrell, *J. Chem. Phys.,* **75,** 5194 (1981).
5. Y. H. Kim and R. P. Wool, *Macromolecules,* **16,** 1115 (1983).
6. R. P. Wool, B. L. Yuan, and O. McGarel, *J. Polym. Eng. Sci,* **16,** 204 (1989).
7. K. Hahn, G. Ley, H. Schuller, and R. Oberthur, *Colloid Polym. Sci.,* **66,** 631 (1988).
8. Ö. Pekcan, M. A. Winnik, and M. D. Croucher, *Macromolecules,* **23,** 2673 (1990).
9. C. L. Zhao, Y. Wang, Z. Hruska, and M. A. Winnik, *Macromolecules,* **23,** 4082 (1990).
10. Y. Wang, C. L. Zhao, and M. A. Winnik, *J. Chem. Phys.,* **95,** 2143 (1991).
11. Ö. Pekcan, M. Canpolat, and A. Göçmen, *Eur. Polym. J.,* **29,** 115, (1993).
12. Ö. Pekcan, M. Canpolat, and A. Göçmen, *Polymer,* **34,** 3319 (1993).
13. M. A. Winnik, M. H. Hua, B. Hongham, B. Williamson, and M. D. Croucher, *Macromolecules,* **17,** 262 (1984).
14. Ö. Pekcan, M. A. Winnik, and M. D. Croucher, *Macromolecules,* **17,** 262 (1984).
15. Ö. Pekcan, M. A. Winnik, and M. D. Croucher, *Phys. Rev. Lett.,* **61,** 641 (1988).
16. Ö. Pekcan, *Chem. Phys. Lett.,* **20,** 198 (1992).
17. M. Canpolat and Ö. Pekcan, *J. Polym. Sci.*, (in press).
18. M. Canpolat and Ö. Pekcan, *Polymer,* **36,** 10,2025 (1995).
19. Ö. Pekcan, *Trends Polym. Sci.,* **2,** 236 (1994).

Received February 11, 1995
Accepted July 30, 1995